Zombies: a simple discrete model of the apocalypse

ABERNETHY, Gavin <http://orcid.org/0000-0001-6983-6349>

CLASSROOM NOTES

Zombies: A simple discrete model of the apocalypse

ARTICLE HISTORY
Compiled October 29, 2018

ABSTRACT
A simple discrete-time two-dimensional dynamical system is constructed and analysed numerically, with modelling motivations drawn from the zombie virus of popular horror fiction, and with suggestions for further exercises or extensions suitable for an introductory undergraduate course.

KEYWORDS
Mathematical modelling, Lyapunov exponents, bifurcation analysis, numerical investigation.

1. Introduction

It is well-documented that discrete-time population models are convenient to handle, display rich dynamic behaviour given their simplicity (see May's classic paper ([1])), and have some reasonable biological justifications ([2]). Bifurcation analysis from dynamical systems theory has proved a popular approach to analysing low-dimensional discrete or continuous models of this kind ([3–10]). By modelling a disease from popular fiction, zombies help to provide a motivation for students to learn about formulating a model from real ecological assumptions, analysing it using the methods of dynamical systems, and then interpreting the physical meaning of their results.

We have previously demonstrated how to investigate a similar population model with cannibalistic tendencies ([11]). Other authors have looked at zombies in particular in varying degrees of detail: Adams' very readable half-novel, half-textbook has a particularly educational focus ([12]); others have performed a serious analysis from an infectious diseases and SIR modelling perspective using a three-dimensional system of ODE's ([13]); and a follow-up study ([14]) further explored the potential for humanity's survival given the slow, undirected movement of zombies that are not well-mixed with the human population by considering the diffusion equation in detail. However, despite this increased attention from the scientific community, we note with concern that Mr Brooks' rigorous text ([15]) is not yet required reading for military or university recruits, and humanity as a whole remains dangerously unprepared for the nightmare that awaits.

This material could be employed as a supplement to a first course in chaos and complex systems, illustrating to students the following skills in applied mathematics:
(a) Formulating and changing a model to reflect various assumptions; simple population dynamics using the logistic map and various common functional responses.

(b) Numerical investigation, with a scientific programming language of choice.
(c) Chaos, strange attractors as well as other kinds of dynamical behaviour in the phase space, Lyapunov exponents, fractals in science/nature by considering the parameter space.
(d) Analysis of dynamical systems by analytically locating and determining the linear stability of fixed points.
(e) Demonstrating the practical application of mathematics to non-specialists, in medical, sociological and ecological fields.

2. Constructing a Simple Discrete Model

We let x_n denote the human population density as a fraction of it's natural carrying capacity in the absence of predators (zombies), and y_n denote the zombie population relative to human density ($0 \leq x_n, y_n \forall n$). Unlike humans, zombies do not require sustenance, mates, water, shelter to maintain their existence, so they do not have a carrying capacity.

Assume that the following occurs, in this order during each timestep:
1. Zombies hunt for humans.
2. The human population undergoes variation in the simplest reasonable manner, according to the logistic map ($x_{n+1} = \alpha x_n(1 - x_n)$).
3. Zombies waste away from natural degredation and accidents. They make no deliberate attempt to protect themselves from environmental hazards.

For the first step, we have a nice advantage here. In addition to the motivational element, zombies are actually ideal predators for an introduction to population dynamics for two reasons: As they are non-sentient, at least in this interpretation, they are unlikely to utilise a sophisticated hunting strategy, prey switching, or require a learning time. This rules out any need for a Holling "Type III" functional response, which lowers the rate of feeding for very low prey populations as the predators try to adapt. Second, as they do not eat for sustenance, there is not going to be a saturation point in terms of the number of human prey, so even a "Type II" response ([16]), which limits the rate of feeding for large prey populations, is unnecessary. To be more precise, we assume that a timestep is sufficiently large that the actual time required to physically consume a caught human is negligible. Together, these assumptions make the choice of the simplest functional response possible, the Lotka-Volterra or unbounded linear functional response $\beta x_n y_n$, seem quite reasonable.

Constructing the model in order, using these three discrete substeps, has two advantages. It is is clear and self-consistent from a modelling perspective, with each action occurring at a certain point. Second, it can model zombie predation taking place constantly over a long time period, during which the human population otherwise remains static, and then the human population subsequently increases with childbirth over a distinct time period short enough to be negligible with respect to zombie feeding. Beginning a given timestep with x_n human density and y_n zombie population, and performing these three steps in order, we obtain:

$$x_{n+1} = \alpha x_n(1-\beta y_n)(1-x_n(1-\beta y_n)) \quad (1)$$
$$y_{n+1} = (1-\delta)y_n(1+\beta x_n) \quad (2)$$

where α is the control parameter for the logistic map, which governs the rate of human reproduction; β is the feeding control parameter which in this case controls the frequency of interaction between humans and zombies (in all cases, this results in the death of the human, who then immediately becomes a zombie); and $0 \leq \delta \leq 1$ is the fraction of the zombie population which perishes each timestep.

To ensure that negative population values are not permitted,

$$x_{n+1} = \Omega\Big(\max\Big(\alpha x_n(1-\beta y_n)(1-x_n(1-\beta y_n)), 0\Big)\Big) \quad (3)$$
$$y_{n+1} = \Omega\Big(\max\Big((1-\delta)y_n(1+\beta x_n), 0\Big)\Big) \quad (4)$$

where

$$\Omega(z) = \begin{cases} z & \text{for } \epsilon \leq z; \\ 0 & \text{otherwise.} \end{cases}$$

Here, ϵ is a minimum population density added for computation purposes so that orbits converging to zero get there in finite time, and can be interpreted as the threshold beneath which there is the equivalent of fewer than one human or zombie.

3. Fixed Points

First, we locate the fixed points of this system. At such points, $x_{n+1} = x_n = x$ and $y_{n+1} = y_n = y$. Therefore,

$$x = \alpha x(1-\beta y)(1-x+\beta xy) \quad (5)$$
$$y = (1-\delta)y(1+\beta x) \quad (6)$$

Solving these simultaneously yields several distinct possibilities:
i) $(x, y) = (0, 0)$
ii) $(x, y) = (x, 0)$. In this case, where there is a non-zero human population but the zombie virus has been completely eradicated, we obtain the solution to the one-dimensional logistic map $x = \alpha x(1-x)$ embedded in the system, which yields $x = 1 - \frac{1}{\alpha}$.
iii) Since if there are no humans, the zombies will all eventually perish (for $0 < \delta$) also, there is no solution lying on the y-axis (i.e. $y = 0 \implies x = 0$), and so the only other solution is (x^*, y^*) where $x^*, y^* \neq 0$. This has the following solution:

$$x, y, \beta \neq 0 \implies x = \frac{1}{\beta}\left(\frac{1}{1-\delta} - 1\right) = \frac{\delta}{\beta(1-\delta)} \quad (7)$$

Hence, since $x \neq 0$:

$$\begin{aligned} 1 &= \alpha(1-\beta y)(1-x(1-\beta y)) && (8)\\ &= \alpha(1-x(\beta y)^2 - x - \beta y + 2\beta x y) && (9) \end{aligned}$$

Solving the quadratic in βy

$$x(\beta y)^2 + (1-2x)(\beta y) + (x + \frac{1}{\alpha} - 1) = 0 \tag{10}$$

yields

$$y = \frac{2x - 1 \pm \sqrt{1 - \frac{4x}{\alpha}}}{2\beta x} \tag{11}$$

Substituting in our solution for x, we obtain:

$$\begin{aligned} x^* &= \frac{\delta}{\beta(1-\delta)} && (12)\\ y^*_{\pm} &= = \frac{2\delta - \beta(1-\delta) \pm \sqrt{\beta^2(1-\delta)^2 - \frac{4}{\alpha}\beta\delta(1-\delta)}}{2\delta\beta} && (13) \end{aligned}$$

3.1. Linear Stability Analysis

We find the Jacobian Matrix of this system. Setting $f(x_n, y_n) = x_{n+1}, g(x_n, y_n) = y_{n+1}$,

$$\begin{aligned} \frac{\partial f}{\partial x} &= \alpha - 2\alpha x + 4\alpha\beta xy - \alpha\beta y - 2\alpha\beta^2 xy^2 = \alpha(1 - 2x - \beta y + 4\beta xy - 2\beta^2 xy^2) && (14)\\ \frac{\partial f}{\partial y} &= 2\alpha\beta x^2 - \alpha\beta x - 2\alpha\beta^2 x^2 y = \alpha\beta x(2x - 1 - 2\beta xy) && (15)\\ \frac{\partial g}{\partial x} &= (1-\delta)\beta y && (16)\\ \frac{\partial g}{\partial y} &= (1-\delta)(1+\beta x) && (17) \end{aligned}$$

Hence, for the fixed point at the origin,

$$J(0,0) = \begin{pmatrix} \alpha & 0 \\ 0 & 1-\delta \end{pmatrix} \tag{18}$$

so the eigenvalues are $\Delta_1 = \alpha$ and $\Delta_2 = 1 - \delta$. Assuming that $0 < \delta < 1$, then this fixed point is stable and attracting when $0 < \alpha < 1$, and a saddle point otherwise.

For the axial fixed point,

$$J(1-\frac{1}{\alpha},0)=\begin{pmatrix}2-\alpha & \beta(\alpha-3+\frac{2}{\alpha})\\ 0 & (1-\delta)(1+\beta-\frac{\beta}{\alpha})\end{pmatrix} \tag{19}$$

and so the eigenvalues are $\Delta_1 = 2-\alpha$ and $\Delta_2 = (1-\delta)(1+\beta-\frac{\beta}{\alpha})$. For this fixed point to be stable and attracting, we require that both $|\Delta_1, \Delta_2| < 1$. The first condition gives $1 < \alpha < 3$, and the second that $|(1-\delta)(1+\beta-\frac{\beta}{\alpha})| < 1$. Let us then consider three possibilities:

- When $0 < \alpha < 1$, we have $1 < \Delta_1$ and $1+\beta-\frac{\beta}{\alpha} < 1$ so $\Delta_2 < 1$. Therefore this is a saddle point if $\frac{\delta-2}{1-\delta} < \beta(1-\frac{1}{\alpha})$ and so $-1 < \Delta_2$, and a repellor otherwise.

- For $1 < \alpha < 3$, $|\Delta_1| < 1$ is satisfied. This prevents the sufficient condition $0 < 1+\beta-\frac{\beta}{\alpha} < 1$ for $|\Delta_2| < 1$ from being fulfilled, so we instead require $0 < \beta(1-\frac{1}{\alpha}) < \frac{\delta}{1-\delta}$ for a stable, attracting fixed point. Otherwise ($\frac{\delta}{1-\delta} < \beta(1-\frac{1}{\alpha})$) it is a saddle point.

- For $3 < \alpha$, we obtain $\Delta_1 < -1$ and $-1 < 0 < \Delta_2$. For a saddle point, we require $\beta(1-\frac{1}{\alpha}) < \frac{\delta}{1-\delta}$ to ensure $\Delta_2 < 1$, and it is a repellor otherwise.

3.2. The Interior Fixed Points for $\delta = 0.1$

Applying the same method of analysis to the interior fixed points is clearly going to be tedious, and this is a motivating factor in turning instead to the methods afforded by computational simulations. However, before we do that we shall study the interior fixed points when $\delta = 0.1$. In general ($0 < \alpha, \beta$ and $0 < \delta < 1$), x^* is always real and positive.

When $\delta = 0.1$, the zombie co-ordinate becomes

$$y^*_{\pm} = \frac{2-9\beta \pm 3\sqrt{9\beta^2-\frac{4\beta}{\alpha}}}{2\beta} \tag{20}$$

Therefore, both solutions are real if and only if

$$9\beta^2 - \frac{4\beta}{\alpha} \geq 0 \tag{21}$$

and since $\alpha, \beta > 0$, this is satisfied for

$$\alpha\beta \geq \frac{4}{9}. \tag{22}$$

We do not require the zombie population to satisfy $y^*_{\pm} < 1$, but we do still require that they are positive. Given that $\alpha\beta \geq \frac{4}{9}$ for the solution to exist, $y^*_+ > 0$ if

$$2-9\beta+3\sqrt{9\beta^2-\frac{4\beta}{\alpha}} > 0 \tag{23}$$

This is immediately satisfied if $\beta < \frac{2}{9}$. If $\beta \geq \frac{2}{9}$ then we require

$$\sqrt{9\beta^2 - \frac{4\beta}{\alpha}} > 3\beta - \frac{2}{3} > 0 \tag{24}$$

and so

$$9\beta^2 - \frac{4\beta}{\alpha} > 9\beta^2 - 4\beta + \frac{4}{9} \tag{25}$$

$$9\beta(1 - \frac{1}{\alpha}) > 1 \tag{26}$$

This inequality then gives two possibilities for $\alpha \neq 1$:
If $0 < \alpha < 1$, this requires that

$$\beta < \frac{1}{9(1 - \frac{1}{\alpha})} < 0 \tag{27}$$

which we discard as we only consider $\beta > 0$, and thus we are left with

$$0 < \frac{1}{9(1 - \frac{1}{\alpha})} < \beta, \text{ for } 1 < \alpha. \tag{28}$$

For $\alpha = 1$, we obtain the condition $z_+ = 2 - 9\beta + 3\sqrt{9\beta^2 - 4\beta} > 0$. This is not real for $0 < \beta < \frac{4}{9}$, and the positivity condition is never satisfied for $\beta \geq \frac{4}{9}$, thus yielding no additional solutions.
Therefore we find that y_+^* is real and positive if:

$$\frac{4}{9\alpha} \leq \beta < \frac{2}{9}, \text{ which requires that } 2 < \alpha. \tag{29}$$

or

$$1 < \alpha \text{ and } \max\left\{\frac{1}{9(1 - \frac{1}{\alpha})}, \frac{4}{9\alpha}\right\} < \beta. \tag{30}$$

However, since $\frac{1}{9(1-\frac{1}{\alpha})} = \frac{4}{9\alpha}$ has only one repeated solution at $\alpha = 2$, we deduce that $\frac{1}{9(1-\frac{1}{\alpha})} \geq \frac{4}{9\alpha}$ throughout the range and so this second possibility simplifies to

$$1 < \alpha \text{ and } \frac{1}{9(1 - \frac{1}{\alpha})} < \beta. \tag{31}$$

For the other fixed point, $y_-^* > 0$ if $\alpha\beta \geq \frac{4}{9}$ for existence and:

$$2 - 9\beta - 3\sqrt{9\beta^2 - \frac{4\beta}{\alpha}} > 0 \tag{32}$$

This requires that $\beta < \frac{2}{9}$, and then that

$$9\beta(1 - \frac{1}{\alpha}) > 1 \tag{33}$$

If $0 < \alpha < 1$, then $\frac{1}{9(1-\frac{1}{\alpha})} < 0$ and we need

$$\beta < \frac{1}{9(1 - \frac{1}{\alpha})} < 0 \tag{34}$$

which has no solutions for $\beta > 0$.
For $\alpha = 1$ then, the fixed point is positive if and only if $z_- = 2-9\beta-3\sqrt{9\beta^2 - 4\beta} > 0$. As with z_+, this has no solutions in the range $\beta \geq \frac{4}{9}$, as illustrated in Figure 1.

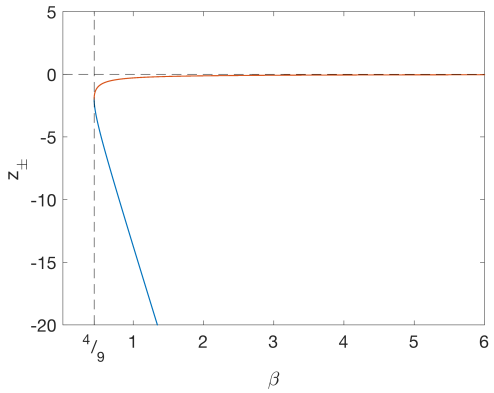

Figure 1. Conditions for $y^*_\pm > 0$ when $\delta = 0.1$, $\alpha = 1$. Red is z_+, blue is z_-.

Finally, for $1 < \alpha$, we need $\frac{1}{9(1-\frac{1}{\alpha})} < \beta$ in addition to $\beta < \frac{2}{9}$. To conclude then, y^*_- is real and positive if:

$$1 < \alpha \text{ and } \max\left\{\frac{1}{9(1 - \frac{1}{\alpha})}, \frac{4}{9\alpha}\right\} < \beta < \frac{2}{9} \tag{35}$$

which requires $2 < \alpha$, and for this range $\frac{4}{9\alpha} \leq \frac{1}{9(1-\frac{1}{\alpha})}$, so we are left with:

$$2 < \alpha \text{ and } \frac{1}{9(1 - \frac{1}{\alpha})} < \beta < \frac{2}{9} \tag{36}$$

as the only suitable region.

To analyse the linear stability of the interior fixed points, rather than explicitly determining the eigenvalues of the Jacobian matrix we instead will use the Jury conditions ([17]). Let $z \in \mathbb{C}$, then defining:

$$F(z) = z^2 - tr(J^*)z + det(J^*), \tag{37}$$

where tr and det denote the trace and determinant, and $J^* = J|_{(x^*,y^*)}$, then $\underline{\mathbf{x}}^*$ is linearly stable if and only if the following conditions are met simultaneously:

$$F(-1) > 0, \quad F(1) > 0, \quad 1 - det(J^*) > 0. \tag{38}$$

Given $\delta = 0.1$ and $x = x^*|_{\delta=0.1} = \frac{1}{9\beta}$, then we obtain:

$$tr(J^*) = \left(\frac{\partial f}{\partial x} + \frac{\partial g}{\partial y}\right)\Big|_{(x^*,y^*)} = \left(\frac{-2\alpha\beta}{9}\right)y^{*2} + \alpha\left(\frac{4}{9} - \beta\right)y^* + \alpha - \frac{2\alpha}{9\beta} + 1 \tag{39}$$

and

$$det(J^*) = \left(\frac{\partial f}{\partial x}\frac{\partial g}{\partial y} - \frac{\partial f}{\partial y}\frac{\partial g}{\partial x}\right)\Big|_{(x^*,y^*)} = \left(\frac{-\alpha\beta}{5}\right)y^{*2} + \alpha\left(\frac{19}{45} - \frac{9\beta}{10}\right)y^* + \alpha\left(1 - \frac{2}{9\beta}\right) \tag{40}$$

Clearly, obtaining analytic solutions to these inequalities is going to be difficult, or impossible. Therefore for each of the two points $(x^*, y^*_{\pm})|_{\delta=0.1}$, in order to understand their stability we shall conduct a numerical search of the two-dimensional (α, β) parameter space and (a) classify regions according to the eight possible combinations of satisfied Jury conditions, and (b) search for boundaries of each of the three conditions.

We perform this procedure for 10,000 values of α in $(0, 5]$ and β in $(0, 6]$ (Figure 2).

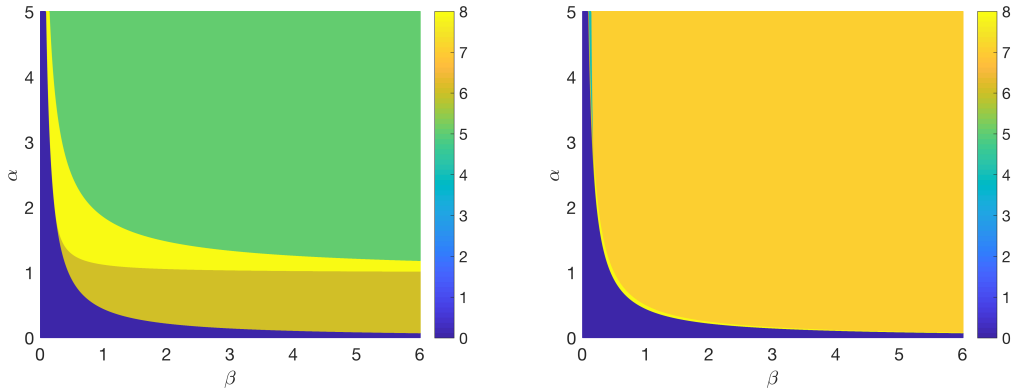

(a) Jury Conditions combinations for y^*_+

(b) Jury Conditions combinations for y^*_-

Figure 2. Purple: Solution is not real and the conditions cannot be evaluated.
Dark Blue (not pictured): $F(-1) \leq 0, \quad F(1) \leq 0, \quad 1 - det(J^*) \leq 0.$
Medium Blue (not pictured): $F(-1) > 0, \quad F(1) \leq 0, \quad 1 - det(J^*) \leq 0.$
Light Blue (not pictured): $F(-1) \leq 0, \quad F(1) > 0, \quad 1 - det(J^*) \leq 0.$
Teal ((b), $\beta \approx 0.25$, $\alpha > 3$): $F(-1) \leq 0, \quad F(1) \leq 0, \quad 1 - det(J^*) > 0.$
Green: $F(-1) > 0, \quad F(1) > 0, \quad 1 - det(J^*) \leq 0.$
Gold: $F(-1) > 0, \quad F(1) \leq 0, \quad 1 - det(J^*) > 0.$
Orange: $F(-1) \leq 0, \quad F(1) > 0, \quad 1 - det(J^*) > 0.$
Yellow: $F(-1) > 0, \quad F(1) > 0, \quad 1 - det(J^*) > 0.$

In the regions where the fixed point exists and could be stable (regardless of whether it takes a biologically-appropriate value), coloured yellow, we see there are three possible ways of leaving this state (aside from changing to complex solutions in the purple region) which correspond to crossing boundaries of different Jury conditions, and giving rise to different types of bifurcation. For y^*_+, if α and β increase

further we enter the green region, passing through $1 - det(J^*) = 0$. This causes the eigenvalues of the Jacobian matrix to leave the unit circle simultaneously as complex conjugates, known as Neimark-Sacker (or Hopf) bifurcation, and resulting in quasiperiodic orbits. If instead α decreases and we enter the gold region, we traverse $F(1) = 0$ and this results in a fold or saddle-point bifurcation as the fixed point, with one real eigenvalue of the Jacobian equal to 1, produces two distinct fixed points. For y^*_-, the main occurence is a period-doubling bifurcation as α and β increase and we enter the orange region by passing $F(-1) = 0$ as a real eigenvalue leaves the unit circle with value -1. There is also the possibility of a saddle-point bifurcation for a narrow band of $\beta \lessapprox 0.2$ and $2 < \alpha$.

By plotting the numerically-identified boundaries of these stability conditions, together with the conditions for existence and positivity located above, we identify the (filled-in green) regions where the fixed points exist, have positive y-coordinate, and possess linear stability (Figure 3).

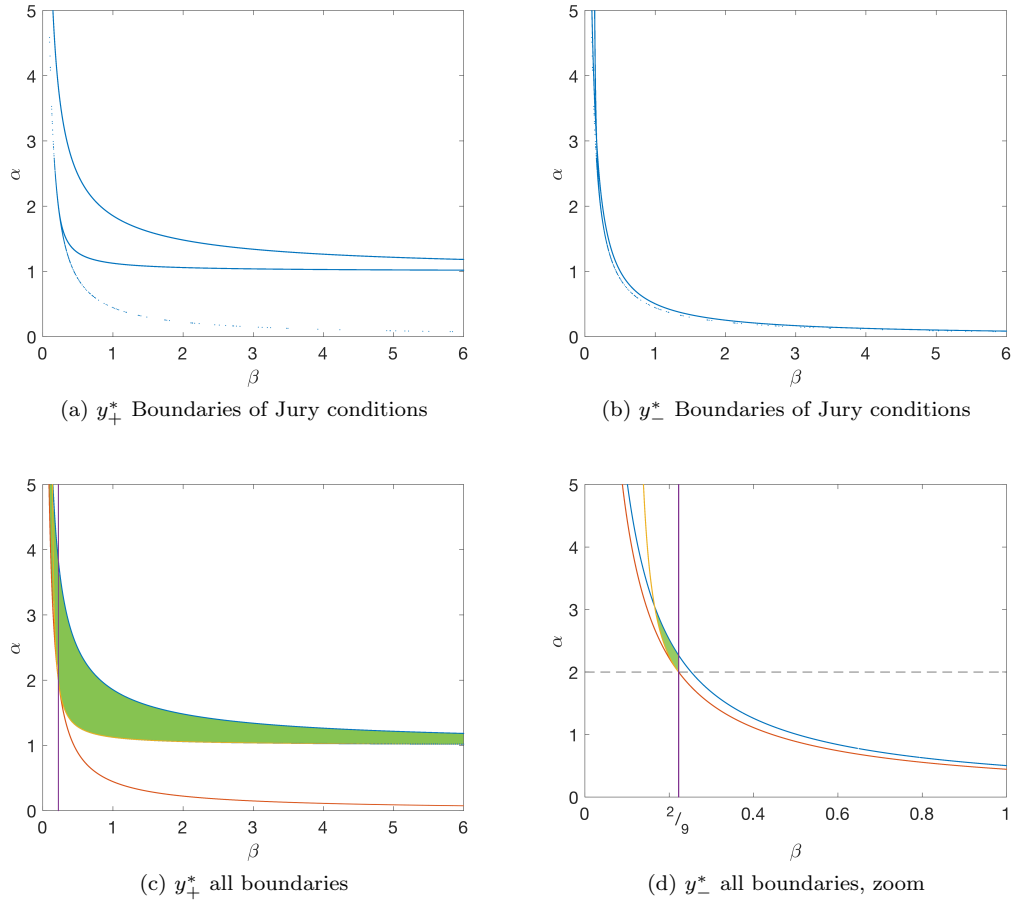

(a) y^*_+ Boundaries of Jury conditions

(b) y^*_- Boundaries of Jury conditions

(c) y^*_+ all boundaries

(d) y^*_- all boundaries, zoom

Figure 3. Boundaries:
Blue = Stability (Jury Conditions),
Red = Existence ($\alpha\beta = \frac{4}{9}$),
Yellow/Purple = Positivity. Yellow denotes $9\beta(1 - \frac{1}{\alpha}) = 1$ and Purple denotes $\beta = \frac{2}{9}$.

We see that the comparatively small region where y^*_- is an attractor (the green region in Figure 3(d)) overlaps with that of y^*_+, so in this case the final behaviour of a given orbit will be determined by the basins of attraction for each interior fixed point.

4. Numerical Analysis of Lyapunov Exponents for $\delta = 0.1$

The spectrum of Lyapunov exponents provide one tool for examining the system through numerical experiments. The maximal or characteristic Lyapunov exponent, λ_1, quantifies the "stretching" of nearby orbits under the action of the map, and so provides a quantifiable measure for the "sensitivity to initial conditions" element of chaotic dynamics. For a discrete orbit $(\underline{\mathbf{x}}_n)_n$ under the map $\underline{f}$, the largest exponent is defined by:

$$\lambda_1 = \lim_{n\to\infty} \frac{1}{n} \sum_{k=0}^{n-1} \ln(|\underline{f}^{'}(\underline{\mathbf{x}}_k)|) \tag{41}$$

However, in order to calculate it practically, we will use the following algorithm found in Sprott's textbook ([18]):
Let

$$J_n = J(\underline{\mathbf{x}})|_{(x_n,y_n)} = \begin{pmatrix} A & B \\ C & D \end{pmatrix} \tag{42}$$

so that A, B, C, D are the entries of the Jacobian matrix evaluated at the nth iteration. Next we define a rescaled variable:

$$y^{'}_{n+1} = \frac{C + Dy^{'}_n}{A + By^{'}_n}. \tag{43}$$

The maximal Lyapunov exponent is then obtained by:

$$\lambda_1 = \lim_{n\to\infty} \frac{1}{2n} \sum_{k=1}^{n} \log\left(\frac{(A + By^{'}_k)^2 + (C + Dy^{'}_k)^2}{1 + {y^{'}_k}^2}\right) \tag{44}$$

We will use the Lyapunov exponent, along with examining whether orbits have settled to a fixed point, to experimentally classify the behaviour of the dynamical system across the (α, β) parameter space for the range $0 \leq \alpha \leq 5$ and $0 \leq \beta \leq 6$ by performing high-precision numerical simulations. Assume that the zombie mortality rate is one tenth of the existing population at each timestep, i.e. $\delta = 0.1$. For each parameter set, we start with a moderate human population density $x_0 = 0.5$ and a small zombie population density $y_0 = 0.01$, and perform 10^5 iterations to remove transient behaviour. This is followed by 10^6 iterations during which the algorithm given above is used to estimate the maximal Lyapunov exponent. As noted in the original set of equations ((3),(4)), if either species' population density falls below $\epsilon = 10^{-6}$ it is considered to have gone extinct and is set to zero.

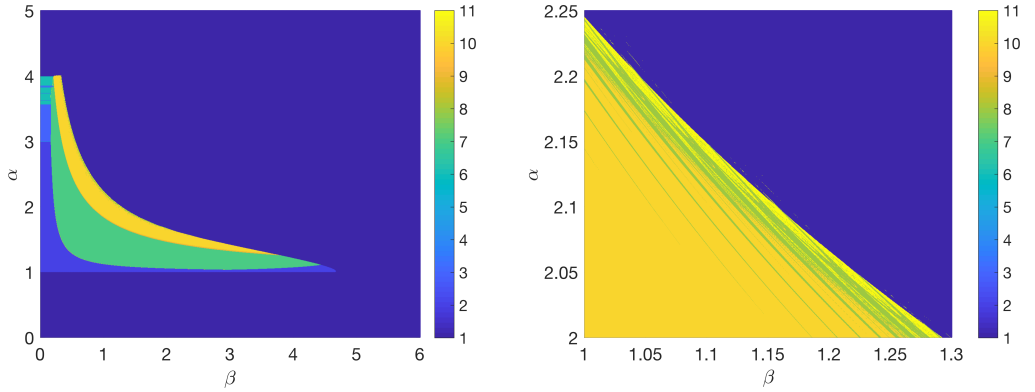

(a) Full (b) Zoom

Figure 4. Qualitative behaviour across the parameter space: Purple = Extinction, Dark Blue = x-only period-1, Medium Blue = x-only periodic, Light Blue (boundary at $\alpha \approx 3$) = x-only $\lambda \approx 0$, Teal (small β, $\alpha > 3.57$) = x-only chaos, Green = Coexistence period-1, Olive Green = Coexistence periodic, Orange = Coexistence quasiperiodicity, Yellow = Coexistence chaos.

Observe (Figure 4) first that the region of either coexistence or human-only survival is bounded. Total extinction occurs if $\alpha < 1$ as the origin is attracting in that region, for $\alpha > 4$ due to the regular behaviour of the logistic map causing x_n to eventually leave the unit interval and thus be set to zero at that or the next iteration, or if α and β are sufficiently large. Like many straightforward discrete-time maps ([19,20]), this model also displays complex two-dimensional dynamics in the parameter space, and the quasiperiodic route to chaos in particular. As α and β increase, the interior fixed point undergoes a Neimark-Sacker bifurcation in accordance with the study of the fixed points' stability in the previous section. If the rotation number of the resulting curve is rational, we land in one of the Arnol'd tongues of periodic behaviour, within which the period-doubling route to chaos occurs. Otherwise, the bifurcation gives rise to a dense ring-like quasiperiodic attractor around the fixed point where $\lambda_1 \approx 0$. Moving further still from the origin, these curves break up and chaotic dynamics are reached regardless. The pattern of Arnol'd tongues themselves form a fractal-like structure in the parameter space, and we note that although too thin to be fully visible, they extend all the way to the boundary with the region of an interior (co-existence) fixed point from which they originate.

Most of the behaviour is therefore explained by our investigation of the fixed points' existence and stability, seemingly combined with total extinctions that (aside from the region where $(0, 0)$ is attracting) is simply due to the biological restraint of discarding populations that map to a negative value at any iteration. This is confirmed by conducting a study of 10,000 values each of α and β in the range, testing whether they escape the range $\mathbb{R}^+ \times \mathbb{R}^+$ within the first 200 timesteps and how rapidly if so (Figure 5).

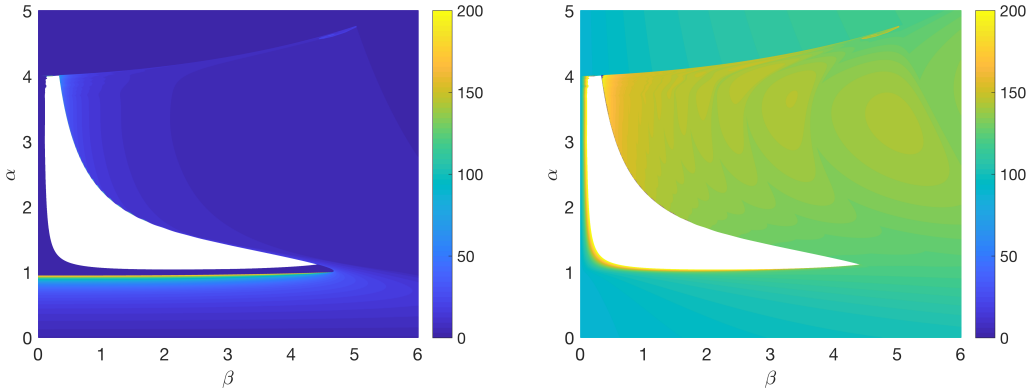

(a) First n for which $x_n \leq 0$

(b) First n for which $y_n \leq 0$

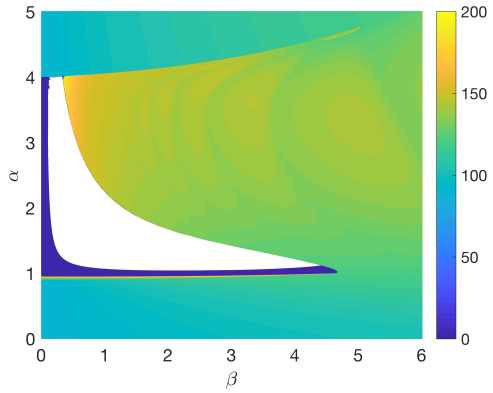

(c) First n for which both $x_n \leq 0$ and $y_n \leq 0$

Figure 5. Escape Sets showing how rapidly orbits with $\delta = 0.1$, $x_0 = 0.5$ and $y_0 = 0.01$ reach $(0, y)$, $(x, 0)$ and $(0, 0)$ within the first 200 iterations

Next, fix $\beta = 0.4$, and we shall consider the behaviour of the largest Lyapunov exponent in more detail. As before, this is calculated over 10^6 iterations after 10^5 transients. This is performed for 100,000 values of $1 < \alpha \leq 4.5$ (Figure 6).

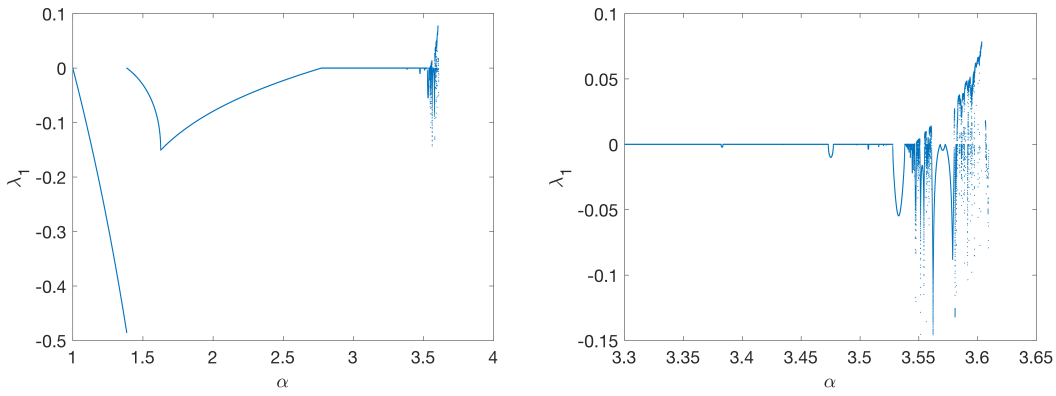

(a) Full

(b) Zoom

Figure 6. Maximal Lyapunov Exponent, $\beta = 0.4$

For this range, we also consider the corresponding bifurcation diagram (Figure 7) of the post-transient dynamic behaviour. This is found by testing the first 1000 iterations for periodicity after 10^8 transients for 20,000 values of $0 < \alpha \leq 5$.

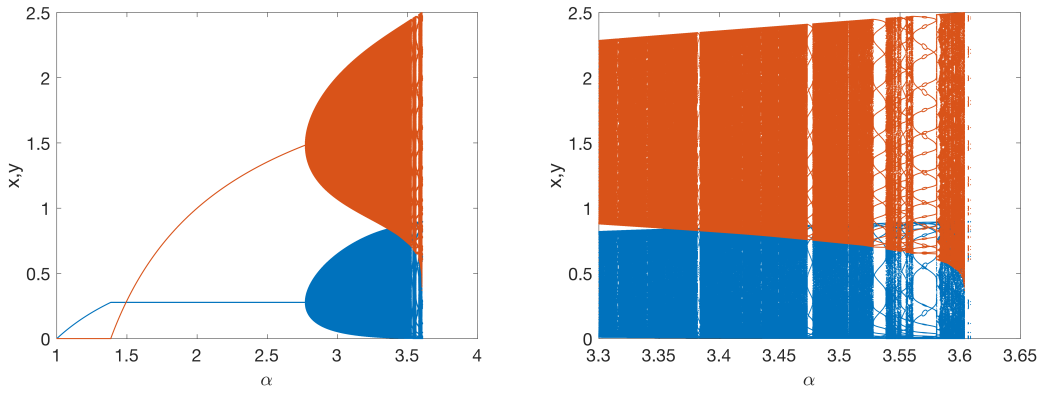

(a) Full (b) Zoom

Figure 7. Feigenbaum diagram, $\beta = 0.4$. Blue = humans, x_n; Red = zombies, y_n.

We see that at $\alpha \approx 2.77$ the largest Lyapunov exponent becomes zero, corresponding to the attractor bifurcating from the fixed point to a quasiperiodic orbit around the point. Periodic windows are observed as we cut into an Arnol'd tongue in parameter space. As with the standard Feigenbaum diagram of the one-dimensional logistic map, in some cases we observe period-doubling to chaos as we remain inside the Arnol'd tongue, for example this is just visible at $\alpha = 3.58$. However, in other cases we instantaneously drop back to quasiperiodic orbits as we exit the Arnol'd tongue in parameter space. This could be used to illustrate the qualitative effects of a predator in introducing entirely new dynamics to the system, that are absent in the one-dimensional case.

Finally, to illustrate this topological relationship between the attractors (Figure 8), we choose three close values of α (keeping $\beta = 0.4$) that give rise to a (a) periodic, (b) quasiperiodic and (c) strange (that is, corresponding to a chaotic orbit) attractors. The difference between (a) and (b) is then simply a matter of their rotation numbers being rational and irrational respectively, and the strange attractor is formed from a twisting of the curve given by quasiperiodic orbits.

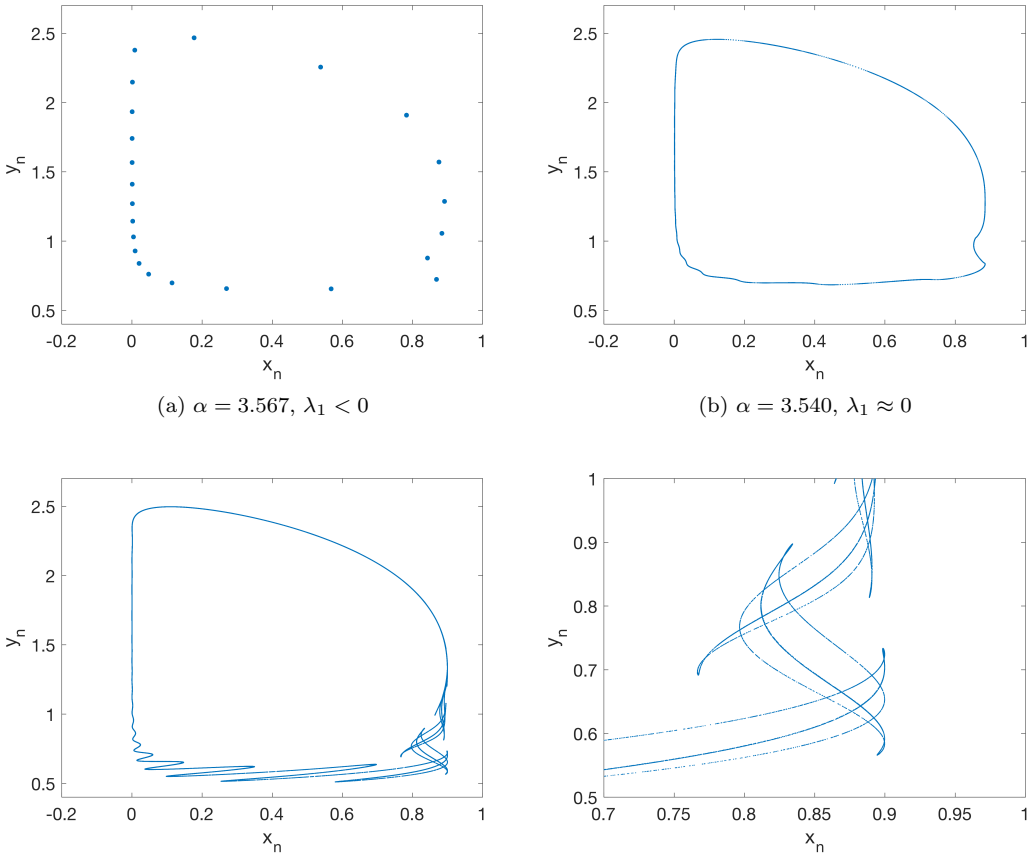

(a) $\alpha = 3.567$, $\lambda_1 < 0$

(b) $\alpha = 3.540$, $\lambda_1 \approx 0$

(c) $\alpha = 3.599$, $\lambda_1 > 0$

(d) $\alpha = 3.599$, zoom

Figure 8. Selection of periodic, quasiperiodic, and strange attractors, for $\beta = 0.4$, $\delta = 0.1$.

5. Conclusion

Whilst this model was not difficult to formulate, it nonetheless illustrated a rich variety of dynamic behaviour and the potential for various avenues of analysis. In fact, because of its intuitive meaning, it is easy propose many changes of varying complexity to the model, by considering different possible interactions between the populations, additional stages of the disease, or even extending to spatial metacommunity of connected cells. In the final section, we suggest some exercises that will test a student's understanding of the biological meaning of the model, and provide opportunities to conduct independent numerical investigations of its dynamics.

6. Exercises

1. Rather than the model derived in equations (1) and (2), consider the simpler population model:

$$x_{n+1} = \alpha x_n(1 - x_n) - \beta x_n y_n \tag{45}$$
$$y_{n+1} = (1 - \delta)y_n + \beta x_n y_n \tag{46}$$

(a) What differences in modelling assumptions are involved in constructing this model?
(b) By means of numerical simulation, investigate the behaviour of this system across the (α, β, δ) parameter space. Do the changes in modelling assumptions significantly alter the likelihood of human survival?

2. What would the set of equations look like if some fraction of the humans caught by zombies are totally consumed rather than successfully converted to joining the zombie population?

3. The discrete Ricker map models reproduction and population dynamics of population desnity x_n using the form:

$$x_{n+1} = x_n e^{\alpha(1-x_n)} \tag{47}$$

(a) What are some advantages and disadvantages of using this form, compared to the discrete logistic map, for the reproduction of the human population?
(b) Reformulate the set of equations for our dynamical system, assuming that the order is preserved but that the humans reproduce according to this map. Numerically investigate the behaviour of this system across the (α, β) parameter space.

4. Suppose the humans organise themselves and start fighting back, so that the zombie mortality rate is now a function of the human and zombie populations.
(a) How would we amend the equations to take into account this new possibility?
(b) Suppose that the new term in this function is directly proportional to the random probability of a human-zombie "collision" (i.e. $\beta \mapsto \beta + \omega x_{n+1} y_{n+1}$). For the parameter space considered, using analytic techniques or numerical simulation, determine how large ω would have to be (i.e. how effective the human hunting parties must be) in order to save the human race at any point in the parameter space which would otherwise result in extinction.
(c) Choose and justify another, more sophisticated response than this linear one.
(d) Instead of this three-step method (zombies hunt, humans reproduce, zombies are hunted by humans and also die naturally), we could assume a simpler model where the humans generally resist an encounter with the zombie. Thus, revert to the plain zombie mortality β, and assume that an encounter during the zombie hunting step now has two possibilities: either the human becomes a zombie or else the zombie is destroyed. Formulate the set of equations corresponding to such a model.
(e) Generalise the equations in (d) to also take into account the possibility of the third outcome to an interaction, discussed in Question 2.

5. Humanity has successfully eradicated this particularly nightmarish strain of the zombie virus, where infection resulted in definite, immediate, conversion to the horde of the dead. However, a new, lesser strain has emerged which has a delay of one time step between infection and, unless treated with probability $\aleph x_{n+1}$ or killed by other causes (with a constant, density-independent probability), becoming a zombie.
(a) Devise a possible set of equations for the three-dimensional parameter space, and be careful to explain the order of occurrences (zombie infection, human reproduction, conversion from infected to zombie etc.) within each time step and ensure that your equations are mutually consistent in this regard.
(b) Why is this version of the model, in the current form at least, fatally flawed?

Consider the timescales of events. (Time to succumb to the disease is equated with an entire human reproductive cycle from conception to, at least, adolescense.)

6. Extending the model to a spatial variant by means of a two-dimensional Coupled Map Lattice ([21–26]) should provide a suitable level of difficulty for a short undergraduate research project. Consider a fully-connected metacommunity of $X_{max} \times Y_{max}$ cells. This affords many modelling possibilities, but we shall choose the following: hunting within cells (based on in-cell population density) is followed by migration of both humans and zombies between adjacent cells at a constant rate μ_x and μ_y respectively. This is then followed by human variation and natural zombie mortality as before.

For a 2×2 metacommunity, where all four cells are adjacent to each other, the equations for this system are as follows:

$$x_{n+1}^{(i,j)} = \alpha\left(\sum_{k=1}^{2}\sum_{l=1}^{2}\mu_x^{(k,l,i,j)}x_n^{(k,l)}(1-\beta y_n^{(k,l)})\right)\left(1-\sum_{k=1}^{2}\sum_{l=1}^{2}\mu_x^{(k,l,i,j)}x_n^{(k,l)}(1-\beta y_n^{(k,l)})\right) \quad (48)$$

$$y_{n+1}^{(i,j)} = (1-\delta)\sum_{k=1}^{2}\sum_{l=1}^{2}\mu_y^{(k,l,i,j)}y_n^{(k,l)}(1+\beta x_n^{(k,l)}) \quad (49)$$

where

$$\mu_x^{(k,l,i,j)} = \begin{cases} 1-3\mu_x & \text{for } i=k, j=l; \\ \mu_x & \text{otherwise,} \end{cases}$$

and similarly for $\mu_y^{(k,l,i,j)}$.

(a) For fixed values of α, β, δ, numerically investigate the effect of the global rates $0 \leq \mu_x, \mu_y \leq \frac{1}{3}$ of human and zombie migration on human survival.
(b) What would the set of equations be if the metacommunity is not fully-connected, and instead, migration can only occur between cells with horizontal or vertical adjacency (i.e. migration between diagonal cells is disabled)? This could be implemented either by changing the double summation's limits to be dependent on the current cell, or simply by altering the migration functions $\mu_x^{(k,l,i,j)}$ and $\mu_y^{(k,l,i,j)}$.
(c) Zombies are unguided hunters who are incapable of strategising. However, humans have some knowledge of their surroundings and do not move randomly. Suggest a more sophisticated migration function for the humans to replace $\mu_x^{(k,l,i,j)}$, so that they try to avoid regions with large zombie populations.

Funding

The author is funded by a grant from the Department for the Economy (https://www.economy-ni.gov.uk/), formerly the Department for Employment and Learning.

References

[1] May RM. Simple mathematical models with very complicated dynamics. Nature. 1976; 26(5560):459–467.

[2] Geritz SA, Kisdi E. On the mechanistic underpinning of discrete-time population models with complex dynamics. J Theor Biol. 2004; 228(2):261 – 269.

[3] Abernethy GM, McCartney M. Analysis of a class of low-dimensional models of mutation and predation. Int J Bifurcat Chaos. 2016; 26(11):1630029.

[4] Agiza H, ELabbasy E, EL-Metwally H, Elsadany A. Chaotic dynamics of a discrete prey-predator model with Holling type II, Nonlinear Anal-Real. 2009; 10(1):116 – 129.

[5] Blackmore D, Chen J, Perez J, Savescu M. Dynamical properties of discrete Lotka-Volterra equations. Chaos Soliton Fract. 2001; 12(13):2553 – 2568.

[6] He Z, Lai X. Bifurcation and chaotic behavior of a discrete-time predator–prey system. Nonlinear Anal-Real. 2011; 12(1):403 – 417.

[7] Hone ANW, Irle MV, Thurura GW. On the Neimark-Sacker bifurcation in a discrete predator-prey system. J Biol Dyn. 2010; 4(6):594–606.

[8] Hu Z, Teng Z, Zhang L. Stability and bifurcation analysis of a discrete predator–prey model with nonmonotonic functional response. Nonlinear Anal-Real. 2011; 12(4):2356 – 2377.

[9] Jing Z, Yang J. Bifurcation and chaos in discrete-time predator–prey system. Chaos Soliton Fract. 2006; 27(1):259 – 277.

[10] Khoshsiar Ghaziani R. Dynamics and bifurcations of a Lotka-Volterra population model. Iran J Sci Technol A. 2014; 38(3):265–279.

[11] Abernethy GM, McCartney M. Cannibalism and chaos in the classroom. Int J Math Educ Sci Technol. 2017; 48(1):117–129.

[12] Adams C. Zombies and Calculus. 2014; Princeton University Press.

[13] Munz P, Hudea I, Imad J, Smith RJ. When zombies attack!: mathematical modelling of an outbreak of zombie infection. Infectious Disease Modelling Research Progress. 2009; 4:133–150.

[14] Smith? R. Mathematical modelling of zombies. 2014; University of Ottawa Press.

[15] Brooks M. The zombie survival guide: Complete protection from the living dead. 2003; Broadway books.

[16] Holling CS. Some characteristics of simple types of predation and parasitism. Can Entomol. 1959; 91:385–398.

[17] Elaydi S. An introduction to difference equations. 2005; Springer Science & Business Media.

[18] Sprott JC. Chaos and time-series analysis. 2003; Vol. 69, Oxford University Press, Oxford.

[19] Elhadj Z, Sprott JC. A minimal 2-d quadratic map with quasi-periodic route to chaos. Int J Bifurcat Chaos. 2008; 18(5):1567–1577.

[20] Kuznetsov YA. Elements of applied bifurcation theory. 2013; Vol. 112, Springer Science & Business Media.

[21] Froyland J. Introduction to chaos and coherence. 1992; CRC Press.

[22] Hassell MP, Comins HN, May RM. Spatial structure and chaos in insect population dynamics. Nature. 1991; 353(6341):255–258.

[23] Hendry R, McGlade J, Weiner J. A coupled map lattice model of the growth of plant monocultures. Ecol Model. 1996; 84(1):81–90.

[24] Huang T, Zhang H, Yang H, Wang N, Zhang F. Complex patterns in a space-and time-discrete predator-prey model with beddington-deangelis functional response. Commun Nonlinear Sci. 2017; 43:182–199.

[25] Lloyd AL. The coupled logistic map: a simple model for the effects of spatial heterogeneity on population dynamics. J Theor Biol. 1995; 173(3):217 – 230.

[26] Solé RV, Bascompte J, Valls J. Nonequilibrium dynamics in lattice ecosystems: Chaotic stability and dissipative structures. Chaos. 1992; 2(3):387–395.